

Type-4 bacterial pili: molecular models and their simulated diffraction patterns

D. A. Marvin^{1*}, K. Nadassy¹, L. C. Welsh¹ and K. T. Forest²

[1] Department of Biochemistry, University of Cambridge, Cambridge CB2 1GA, UK

[2] Department of Bacteriology, University of Wisconsin, Madison WI 53706, USA

*Corresponding author: d.a.marvin@bioc.cam.ac.uk

Fibre Diffraction Review **11**, 87-94, 2003

ABSTRACT

Bacterial pili are long thin assemblies of pilin protein subunits, that extend outwards from the surface of bacteria and are involved in interaction of bacteria with their environment, notably attachment of pathogenic bacteria to their host and "twitching motility" of bacteria along surfaces. Pili are about one-third the diameter of bacterial flagella. Some types of pili are the adsorption sites of filamentous bacteriophage. X-ray fibre diffraction patterns of type-4 pili are classical α -helix patterns, with strong intensity in the equatorial direction at about 10 Å and in the meridional direction at about 5 Å. The crystal structure of the type-4 pilin subunit has a highly conserved ~50-residue N-terminal α -helix and a less conserved ~100-residue globular C-terminal domain, and this subunit structure has been used to construct models of type-4 pili in which the N-terminal α -helix of the pilin forms the central core of the pilus. We find that the calculated fibre diffraction patterns predicted for these models are less similar to the observed diffraction patterns than diffraction patterns predicted for models built from only the N-terminal α -helix portion of the subunit. Twitching motility and phage infection proceed by retraction of pili, probably involving dissolution of pilin at the base of the pili into the host cell membrane, reminiscent of the process of filamentous phage infection by disassembly of the phage subunits into the membrane.

Introduction

Pili are filamentous polymers of protein subunits extending from the surface of Gram-negative bacteria. They are about 50-100 Å in diameter, depending on the type of pili, significantly thinner than bacterial flagella. Many different types of pili have been identified. Pili of one type, type 4 pili (Tfp) have been extensively studied, especially because of their medical importance. Tfp interact with target mammalian cells in the first step of bacterial infection. They function in part by 'retraction': after the pilus attaches to the target, it withdraws into the bacterial cell, probably by depolymerization of the pilin subunits at the base of the pilus into the bacterial inner membrane, thereby drawing the bacterium to the attachment site. This retraction mechanism is also involved in 'twitching motility' of bacteria across surfaces, and in the infection mechanism of some filamentous bacteriophages. (For reviews see [1-5]).

X-ray fibre patterns of PAK and PAO Tfp from *Pseudomonas aeruginosa* bacteria show the strong 10 Å equatorial and 5 Å meridional intensity typical

of α -helix assemblies [6]. These patterns also show orders of an apparent 41 Å layer-line periodicity. The determination of the crystal structure of the pilin subunit of MS11 Tfp from *Neisseria gonorrhoeae* bacteria [1,7,8] has opened the way for a major advance in the analysis of pili structure. The MS11 pilin has a ca. 50-residue α -helix at the N-terminus, a region that is highly conserved across different Tfp, and a ca. 100-residue globular four-stranded antiparallel β -sheet region at the C-terminus, a region that is less conserved. The structure of the globular region of *Ps. aeruginosa* pilin has been determined by x-ray crystallography for PAK pilin [9] and by NMR for K122-4 pilin [10], and has a largely β -sheet structure homologous to the corresponding region of MS11, but with some differences in the fold of the polypeptide chain. One would like to build the high resolution pilin structure into the symmetry determined from the lower resolution fibre patterns of pili, and thereby to determine how the pilin molecules are packed within the pilus filament. The proposal that the α -helix portions of pilin molecules pack together at the core of the pilus with the globular portion on the outside (7) is probably correct in general, but there are some

limitations to the current fibre diffraction data, and therefore there is some uncertainty about the details of the pilus helix parameters and even the hand of the pilus helix.

Materials and Methods

Experimental fibre diffraction. PAK pili were prepared and purified from *Pseudomonas aeruginosa* type K [6]. PAK fibre F28A was prepared by Dr. Waltraud Folkhard. A 3 μl drop of a 100 mg/ml gel of purified pili was suspended between the tips of two glass rods about 1.6 mm apart and dried under humidity control over 10 days; the fibre was stretched slightly several times during the first 5 days. The fibre was then stored for 20 years at room temperature and humidity. MS11 pili were prepared and purified as described [11], and fibres were prepared essentially as for PAK. Each fibre was dusted with Si powder to give a calibration ring at 3.136 \AA , and diffraction patterns were obtained at the Synchrotron Radiation Source, Daresbury Laboratory on station 7.2 with a wavelength of 1.488 \AA , at room temperature and humidity. See [12-15] for further details of our diffraction methods.

Building models and calculating simulated diffraction patterns. To generate coordinates of a reconstituted full PAK pilin molecule, we superimposed residues 30 to 51 of the truncated PAK model 1DZO [9] onto the corresponding residues of the MS11 model 2PIL [8], and added the coordinates of residues 1 to 30 of 2PIL to those of residues 31 to 144 of 1DZO. We then applied the matrix given for 2PIL [8] to move this model into the frame of reference of the pilus helix. We then applied integral multiples of the appropriate [unit twist, unit rise] (e.g., [72°, 8.2 \AA] for a 5 units/turn right-handed helix) to generate a segment of pilus. When displaying the pilus models, we truncate at upper and lower axial (z) values, to give a representation of a slab sliced from a long pilus. For other types of model, we generated residues 1 to 50 as gently-curved α -helices with various orientations and shapes using the methods developed for filamentous phage [13]. We based some of our models on unpublished model-building studies of PAK carried out by Dr. Tania Watts at EMBL Heidelberg in 1981-1982; see also [6,16,17].

In the region of the diffraction pattern corresponding to spacings greater than about 10 \AA , the reduced

contrast between the solvent and the molecule reduces the observed diffracted intensity relative to that expected for a molecule in vacuum. We calculated the helix transform of the pilus including the solvent as described for filamentous bacteriophage [14]. We generated simulated fibre diffraction patterns from the calculated continuous molecular transform essentially as described [14], but using the program LSQINT (www.ccp13.ac.uk) to generate the simulated diffraction pattern to a reciprocal space radius of 0.32 \AA^{-1} . We did not model the observed crystal lattice sampling in the inner equatorial region, so all our simulated patterns show strong J_0 transform in this region, which can be disregarded.

Fibre diffraction patterns generally show lines of intensity, the layer lines, and measuring the positions of these lines gives information about the helix parameters. On the PAK patterns, there is a clear layer line at 41 \AA , with near-meridional intensity, and we take this as the helix pitch [6]. Better-aligned patterns would enable the distribution of continuous transform intensity along the layer lines to be measured and compared quantitatively with the intensity distribution predicted by models. If intensity changes due to heavy-atom derivatives can be measured, these intensity changes could give further information about the helix parameters.

There are various types of disorder that can smudge out layer lines. These include disorientation (not all filaments in the fibre lie parallel to one another) and limited coherence length (the regular helix extends for only a short distance along the filament). These two kinds of disorder can be modelled with the CCP13 program LSQINT, so given a hypothesis about the structure and about the nature of the disorder in the fibre pattern, one can model the predicted diffraction pattern and compare it with the observed diffraction pattern. After several trials for disorder in our simulated PAK diffraction patterns, we chose the width of the disorientation distribution (awid) as 13° and the coherence length (1/zwid) as 500 \AA . There are other kinds of disorder that are not so easy to model, for instance the helix parameters may vary along the length of the pilus, so slightly different helix diffraction patterns are superimposed.

Units per turn. In order to build any detailed model, it is necessary to know the 'unit rise' of the helix; that is, the average distance from one subunit to the next along the helix axis. It is seldom possible to

determine this directly from the fibre diffraction data. Instead, one can determine, in separate experiments, the mass of the subunit and the mass per length of the helix. Then unit rise = (mass of subunit)/(mass per length of helix). The number of 'units per turn' (u/t) = (helix pitch)/(unit rise). Note that in principle u/t need not be integral, but a non-integral u/t will affect the pattern of layer lines, and the analysis of the PAK and PAO pili diffraction patterns [6] suggests that u/t is integral or near-integral. We take the helix pitch in this case as defined by the 41 Å near-meridional reflexion on the PAK fibre patterns. In 1981, neither the mass of the pilin subunit nor the mass per length of the pilus was known accurately. To determine the volume of the pilus repeat, the side a of the hexagonal unit cell in the fibre was measured as a function of water content of the fibre, and extrapolated to zero water content. These measurements are accurate to better than 1%, and have an internal control, a crystal powder on the fibre that gives a calibration ring of known spacing. Both PAK and PAO extrapolate to $a = 52$ Å at zero water content [6]. The cross-sectional area of a hexagonal unit cell with $a = 52$ Å is 2342 Å². The volume of the pilin was estimated from the amino acid composition and estimates of amino acid volumes, as described for filamentous phage [12], and for 41 Å pitch, the calculation [6] gave $u/t = 4$. The molecular weight determined from the sequence [17] was found subsequently to be about 20 % smaller than previously estimated, so the estimate of u/t for PAK was increased from 4 to 5 [17]. This estimate was also used for molecular models of MS11 pili [7,8].

To get a better (but still poor) estimate of u/t for PAK, we have calculated the volume of a PAK pilin subunit reconstructed from the PAK globular portion and the MS11 α -helix portion, using VOIDOO [18] with a 0.4 Å probe radius (this radius, which is smaller than the 1.4 Å usually used in calculating water exclusion, was chosen by analogy with the value found for Pf1 filamentous phage [12]), giving 1.90×10^4 Å³ for the volume of PAK pilin, so for a 41 Å pitch, $u/t = 5.1$. For MS11 we have not yet taken diffraction patterns at a series of water contents, but we used the value $a = 55.9$ Å from a pattern taken at low humidity. The cross-sectional area of the unit cell is then 2706 Å². Using VOIDOO we calculate 2.14×10^4 Å³ for the volume of MS11 pilin, so for a 41 Å pitch, $u/t = 5.2$. We have tried both $u/t = 4$ and $u/t = 5$ in our model building, and

left-handed as well as right-handed pilus helices. As found for filamentous phage, an integral change in the number of units per turn, or reversing the hand of the helix, makes little difference to the low resolution simulated diffraction pattern. If there are fewer units per turn the subunit will be at a smaller radius, to maintain the packing density, and contacts between overlapping subunits separated by one pitch length in the axial direction can be maintained by changing the slope of the α -helix [13].

Once one knows the helix symmetry, has well-resolved layer lines, and has measured the intensity distribution along the layer lines, one could use automatic refinement methods, as a kind of molecular replacement, to build the pilin molecule into the pilus symmetry. This would require fitting the molecular transform of the subunit to the observed fibre data, including stereochemical constraints with the possibility of some flexibility within the subunit, especially in the α -helix rod. This kind of automated refinement would require that the initial model be within the radius of convergence of the refinement method, and would work best when the helix parameters are known with certainty. We are not yet at this stage of the structure analysis, and our models must be considered as very preliminary.

A note on nomenclature: in fibre diffraction, the word 'fibre' refers to the macroscopic bundle of filaments that is put into the X-ray beam, analogous to 'crystal' in protein crystallography. Some authors have used 'fibre' to refer to the individual pilus, but this can lead to confusion, and it is better to use 'filament' or 'fibril' or indeed 'pilus' to refer to the individual pilus.

Results

Our fibre diffraction patterns of PAK and MS11 (Figure 1) are similar to those previously reported [6] for PAK and PAO pili. There is strong equatorial and near-equatorial intensity at about 10 Å, and strong meridional intensity at about 5 Å, suggesting a substantial fraction of α -helix oriented at a small angle to the fibre axis. There is meridional and near-meridional intensity that can be indexed as orders of a 41 Å layer-line spacing. (As pointed out [6], this spacing increases slightly with increased humidity, from about 39 Å to about 41 Å). But the MS11 pattern shows several interesting differences in detail from that of PAK. There is off-meridional intensity that cannot be indexed on the 41 Å layer-line

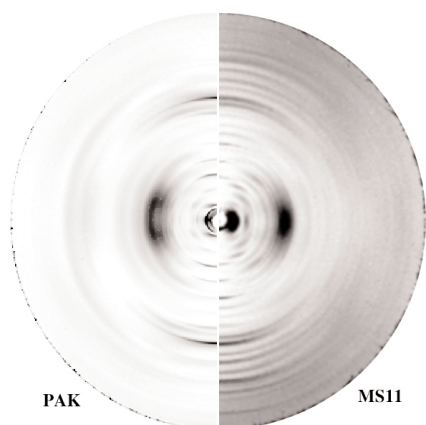


Figure 1. X-ray fibre patterns of type 4 pili. Left, PAK, fibre number F28A; right, MS11. Patterns are shown in detector space. Fibre axis is vertical. The outer radius of the patterns is about that of the calibration ring (about 3.1 Å).

spacing, suggesting the possibility of a pilus helix with a non-integral number of units per turn in the 41 Å repeat. Moreover, the 10 Å equatorial region of PAK is stronger on $l = 1$ than on the equator ($l = 0$), whereas the corresponding region of MS11 seems strongest on $l = 0$. These differences in detail are reminiscent of differences between fibre patterns of class I and class II filamentous bacteriophage [12,14] that result from differences in packing of otherwise similar subunits within the bacteriophage helix [19]. The differences between the MS11 and PAK diffraction patterns suggest the possibility of interesting differences between the assembly of these otherwise similar proteins. However, in the absence of detailed data, we follow ref. [7] in applying the helix parameters of PAK to the preliminary analysis of MS11.

Modelling the pilus structure. At low resolution, the pilin can be considered as an α -helix rod with a globular portion at the C-terminal end. The position and orientation of the rod is fairly well defined by the 10 Å equatorial and near-equatorial intensity, and this will not be significantly affected by variation in the pilus helix parameters. There is little higher resolution off-meridional detail, suggesting that the globular portion does not contribute much to the diffraction pattern.

To test the validity of PAK models, we calculated simulated diffraction patterns to compare with the observed PAK diffraction pattern. As a first trial, we used the coordinates 1DZO of the PAK globular domain, spliced to the α -helix domain of the 2PIL MS11 model, and transformed into the position of a subunit in the MS11 helix using the matrix given in PDB entry 2PIL. The orientation of the globular

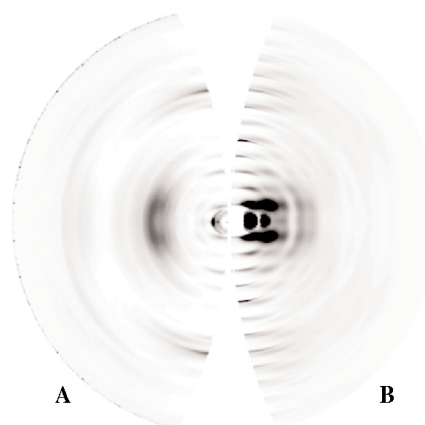


Figure 2. A. Observed diffraction pattern of PAK pili, transformed to reciprocal space. B. Simulated fibre diffraction pattern of a PAK model, residues 1 to 50 of 2PIL (MS11) combined with residues 51 to 144 of 1DZO (PAK) and transformed into the frame of reference of the pilus helix using the matrix and vector given in PDB entry 2PIL. Both the simulated and the observed patterns extend to about 3.1 Å.

domain with respect to the pilus axis is unchanged by this transformation, and in particular the hydrophobic residues still face inwards, and pack against the hydrophobic α -helix. The simulated diffraction pattern of this model has several flaws (Figure 2). There is little predicted intensity at the 10 Å equatorial position; and there is detailed predicted intensity on higher layer lines, even after applying corrections for disorder, whereas little detail is present in this region on observed patterns. Also the pattern of calculated intensity on the meridional series of reflexions is not the same as on the observed pattern. The absence of the 10 Å intensity suggests that the orientation and/or packing of the α -helix rod needs to be altered; and the calculated detail on higher layer lines suggests that further (not modelled) disorder may be present. The poor simulated pattern is not just a consequence of combining information from PAK and MS11 crystal structures, since we find that a simulated diffraction pattern of a preliminary pure MS11 model also is a poor fit to the observed MS11 pattern (calculation not shown).

The MS11 subunit α -helix domain is rather twisted, and in the MS11 pilus model the neighbouring α -helices are not in regular close contact along their length (see Figure 1 of ref. 1). The 10 Å equatorial region of an α -helix diffraction pattern arises from close packing of the 10 Å-diameter α -helices, and the curvature of the MS11 subunit prevents close packing. But an extended free-standing α -helix is relatively flexible and can be bent without distorting the internal stereochemistry. Thus we modelled the

packing of the α -helix portion separately from the globular portion, and attached the globular portion after the α -helix packing was established. We used the methods developed for building models of the filamentous phage subunit [13,19] to build a gently-curved α -helix domain with the sequence of PAK residues 1 to 50; the shape and orientation of the subunit in the pilus were chosen to give good local packing between α -helices. We added this to the globular domain, to generate a new model of the PAK pilus (Figure 3). The α -helices are close-packed in the 0-5 direction, that is, parallel to the pilus axis, between subunits separated by one turn of the 41 Å pitch pilus helix, but they are not as close-packed in other directions. The simulated diffraction pattern of this model (Figure 4) has a stronger 10 Å equatorial region than that of Figure 2, but is still flawed in other ways, especially in predicting non-observed diffracted intensity.

We considered that the globular domain of the subunit might be substantially disordered, but we were unable to improve the simulated diffraction pattern by modelling this disorder, either by increasing the temperature factor of the atoms in residues 51 to 144 to $B = 100 \text{ \AA}^2$, or by replacing the globular domain by a low resolution diffuse electron density distribution. Fibre diffraction patterns of PAK pili studied as a function of water content over the range 0% to 98% relative humidity show an increase in unit cell volume of 50% but no appreciable increase in order [6], so the absence of order is unlikely to be due to distortion of the pilus surface as a result of close packing in dry fibres. We also tried models with $u/t = 4$ rather than $u/t = 5$, and left-handed rather than right-handed pilus helices, but these models also gave simulated diffraction

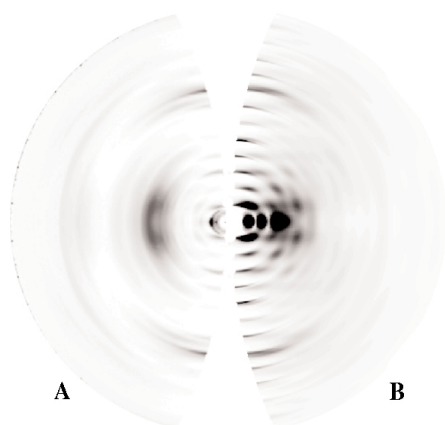


Figure 4. **A.** Observed diffraction pattern of PAK pili, transformed to reciprocal space. **B.** Simulated fibre diffraction pattern of the PAK model of Figure 3.

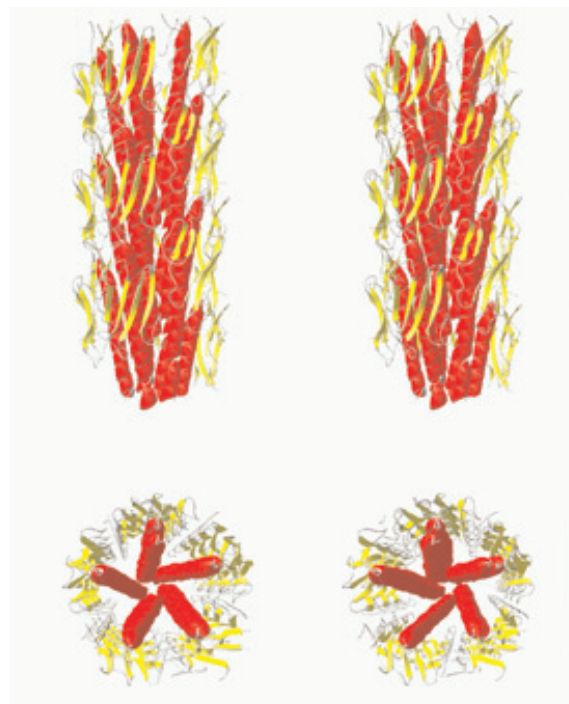


Figure 3. Model of PAK. Residues 1 to 50 of a gently-curved α -helix (with the MS11 sequence) were combined with residues 51 to 144 of 1DZO (PAK) and transformed into the frame of reference of the pilus helix using the matrix and vector given in PDB entry 2PIL. Ribbon representation. The α -helix is in red and the β -sheet in yellow. Slab 100 Å long in the axial direction. Stereo pairs. **Top:** view from the side of the pilus. **Bottom:** view down the axis of the pilus. This figure was prepared using Swiss-PdbViewer [26] (www.expasy.org/spdbv).

patterns with low intensity in the 10 Å equatorial region where observed intensity is strong, and high intensity in regions where observed diffraction is weak. Only one type of model gave a simulated diffraction pattern that looks similar to the observed: a model with the globular domain entirely removed, and the longer sidechains on the α -helix replaced by Ser, effectively assuming that everything except the

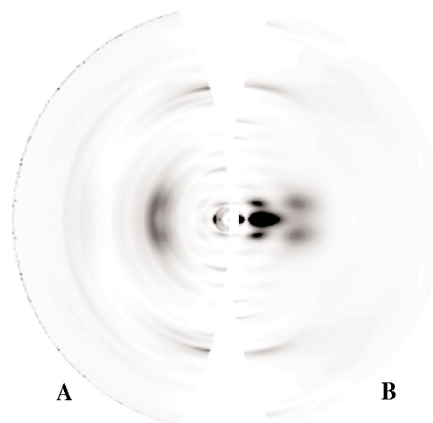


Figure 5. **A.** Observed diffraction pattern of PAK pili, transformed to reciprocal space. **B.** Simulated fibre diffraction pattern of the α -helix region only (residues 1 to 50) of the PAK model of Figure 3, with the larger sidechains replaced by Ser.

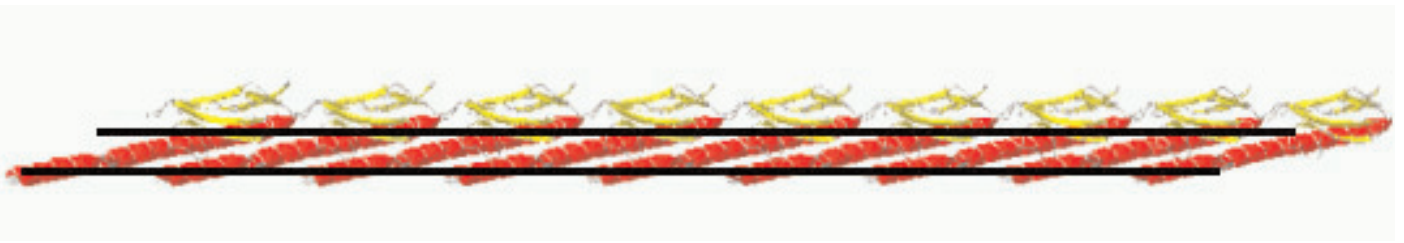


Figure 6. The subunits of a single 0 to 5 helicoid of the model of Figure 3 were generated by translating the subunit parallel to the pilus axis by integral multiples of 41 Å, and the assembly was rotated to represent a horizontal layer in the membrane. The thick black lines are about 25 Å apart, and represent the thickness of the hydrophobic region in the lipid bilayer. The globular C-terminal region at the top is in the periplasmic space, and the N-terminus of the α -helix region is in the cytoplasm [2].

α -helix backbone is so disordered that it blends into the solvent background (Figure 5). This type of model is reminiscent of "intrinsically disordered" regions in some globular proteins [20], although NMR solution studies of the globular domain of the K122-4 strain of *Ps. aeruginosa* Tfp pili do not suggest any unusual disorder [10].

From native fibre diffraction data alone one cannot determine the hand of the pilus helix, or the direction in which the α -helix wraps around the pilus helix axis. Models of different hands (but otherwise unchanged) are indistinguishable at low resolution. Moreover, instead of interpreting the 41 Å repeat as the pitch of a 5 units per turn helix, one could say that it corresponds to a group of 5 subunits related by a 5-fold rotation axis that coincides with the pilus axis. Such a model predicts meridional reflexions every 41 Å, which are not observed, although there could be special reasons for their absence. It is also conceivable that the asymmetric unit in the pilus helix is a pair of pilin subunits, related by a diad, as found for isolated pilin solubilised in octyl glucoside [17], and as found in the crystal structure [7], but this type of model would raise difficult questions about the mechanism of pilus assembly.

Discussion

Despite the imperfections in our model of pili, we can make some hypotheses about pili assembly and pili retraction. Possible mechanisms for pili retraction have been discussed [2-5,21]. Two separate questions arise: the nature of the retraction mechanism, presumed to occur at the base of the pilus; and the way in which the attachment of the pilus outer tip to the target transmits a signal to the base, to activate the retraction mechanism.

We propose a model for the assembly and retraction of pili that is based in part on the model for assembly of filamentous bacteriophage from α -helical subunits

that reside in the bacterial inner membrane before assembly [22]. Assembly of filamentous bacteriophage and Tfp are both examples of the type II secretion system, involving assembly at the inner membrane followed by transport through a pore in the outer membrane [23]. Our model makes use of a fact from differential geometry, that a toroid can be deformed into a helicoid with no deformation of local geometry (for instance, see mathmuse.sci.ibaraki.ac.jp/deform/DeformationE.html). One can draw a set of helicoids through the α -helix axes of the pilin subunits in the Tfp model of Figure 3. One of these helicoids is illustrated in Figure 6. If the pilin subunits in the membrane pre-assemble side-by-side into ribbons in the membrane, then a set of these ribbons could twist out of the membrane into the pilus with little change in local contacts within the ribbon (Figure 7). For pilus retraction, the

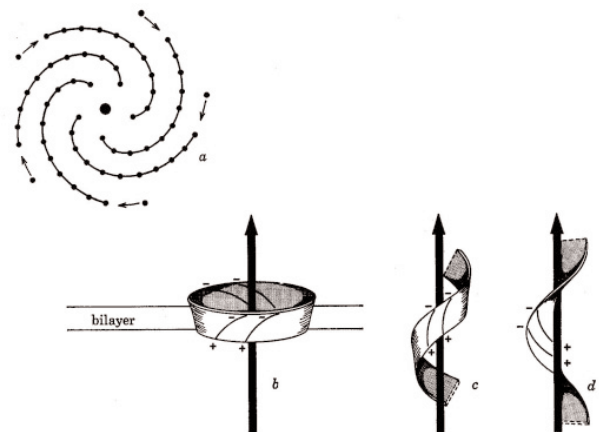


Figure 7. Schematic representation of how a set of ribbons in the membrane can be transformed into a set of helicoids in the pilus with minimal local distortion of the contacts between pilin subunits within the ribbon. (a) Top view of pilin in the membrane; dots represent individual pilin subunits, pre-assembled with contacts between α -helices within the membrane being the same as within the 0-5 ribbons of the pilus. (b-d) Transformation of a catenoid (b) to a helicoid (d). The catenoid, slit down one side and opened out, would correspond to one of the spirals in (a); the helicoids would correspond to one of the 0-5 ribbons in the pilus. The individual subunits are represented as curves on the ribbon; the (+) signs represent the N-terminus and the (-) signs represent the C-terminus. (After [22]).

helicoids would convert back into ribbons in the membrane. The hydrophobic contacts between adjacent ribbons in the pilus would not be the same as the hydrophobic contacts between ribbons and lipids in the membrane, but they would be similar. A slight change in the helix parameters of the pilus, as a result of specific binding at the pilus tip, for instance like the transition caused by a slight temperature change of Pf1 filamentous phage [15], might change the contacts between ribbons in the pilus sufficiently to change the entropically favoured structure from 'ribbons in pili' to 'ribbons in membrane'. This mechanism could be classed as a 'Brownian ratchet' [5,21]. The random Brownian motion of the ribbons would be rectified in one direction or the other by the difference in entropy between the 'ribbons in the membrane' and the 'ribbons in pili'. This model for pili assembly and retraction does not depend on the details of our structural model for pili, but only on the general feature that α -helices are close-packed at the core of the pilus.

Conclusions

We need an accurate determination of mass/length, to combine with the known mass of the pilin subunit, to decide the number of units per turn in PAK and MS11 pili, to be able to build detailed models of pili. We need better quality fibre diffraction patterns of native and mutant pili of the various types, especially MS11 and PAK. The relatively poor quality of the fibre diffraction patterns suggests disorder, and the effects of various kinds of disorder can be analysed theoretically [24,25], but it is likely to be more productive to search for experimental methods to reduce this disorder. One needs to try many different conditions for making fibres: chemical (salt, pH, non-ionic detergents, in vitro reassembly); physical (temperature, shear, magnetic field, electric field); and biological (different natural strains; constructed mutants in the pilin sequence which might affect the alignment in the fibre, for instance mutants that form rigid pili, or pili that aggregate less readily; mutants that hyperproduce pili). In some ways surveying fibre formation is more difficult than surveying conditions for crystallizing a protein, because one usually gets a fibre no matter what the conditions, and one needs to take a diffraction pattern of every fibre to see its quality. Mutants of pili could be surveyed for altered morphology by electron microscopy in the first instance. Image reconstruction from electron micrographs of

unstained samples imbedded in ice might be another approach to determine the relation between pilin molecules in the pili, but fibre diffraction has the potential to give higher resolution data than electron microscopy.

Acknowledgements

This research was funded in part by a grant from The Wellcome Trust to Professor R.N. Perham, and we thank Professor Perham for his support.

References

- [1] Forest, K. T. & Tainer, J. A. (1997) Type-4 pilus-structure: outside to inside and top to bottom—a minireview. *Gene* **192**, 165-169.
- [2] Wolfgang, M., van Putten, J. P. M., Hayes, S. F., Dorwald, D. & Koomey, M. (2000) Components and dynamics of fibre formation define a ubiquitous biogenesis pathway for bacterial pili. *EMBO J.* **19**, 6408-6418.
- [3] Kaiser, D. (2000) Bacterial motility: How do pili pull? *Current Biology* **10**, R777-R780.
- [4] Skerker, J. M. & Berg, H. C. (2001). Direct observation of extension and retraction of type IV pili. *Proc. Natl. Acad. Sci. USA* **98**, 6901-6904.
- [5] Merz, A. J. & Forest, K. T. (2002) Bacterial surface motility: Slime trails, grappling hooks and nozzles. *Current Biology* **12**, R297-R303.
- [6] Folkhard, W., Marvin, D. A., Watts, T. H. & Paranchych, W. (1981) Structure of polar pili from *Pseudomonas aeruginosa* strains K and O. *J. Mol. Biol.* **149**, 79-93.
- [7] Parge, H. E., Forest, K. T., Hickey, M. J., Christensen, D. A., Getzoff, E. D. & Tainer, J. A. (1995). Structure of the fibre-forming protein pilin at 2.6 Å resolution. *Nature* **378**, 32-38.
- [8] Forest, K. T., Dunham, S. A., Koomey, M. & Tainer, J. A. (1999) Crystallographic structure reveals phosphorylated pilin from *Neisseria*: phosphoserine sites modify type IV pilus surface chemistry and fibre morphology. *Molecular Microbiology* **31**, 743-752.
- [9] Hazes, B., Sastry, P.A., Hayakawa, K., Read, R. J. & Irvin, R. T. (2000) Crystal structure of *Pseudomonas aeruginosa* PAK pilin suggests a main-chain-dominated mode of receptor binding. *J. Mol. Biol.* **299**, 1005-1017.
- [10] Keizer, D. W., Slupsky, C. M., Kalisiak, M., Campbell, A. P., Crump, M. P., Sastry, P. A., Hazes, B., Irvin, R. T. & Sykes, B. D. (2001) Structure of a pilin monomer from *Pseudomonas aeruginosa*. *J. Biol. Chem.* **276**, 24186-24193.
- [11] Forest, K. T., Bernstein, S. L., Getzoff, E. D., So, M., Tribbick, G., Geysen, H. M., Deal, C. D. & Tainer, J.A. (1996) Assembly and antigenicity of the *Neisseria gonorrhoeae* pilus mapped with antibodies. *Infect. Immun.* **64**, 644-652.
- [12] Nave, C., Brown, R. S., Fowler, A. G., Ladner, J. E., Marvin, D. A., Provencher, S. W., Tsugita, A., Armstrong, J. & Perham, R. N. (1981). Pf1 filamentous bacterial virus. X-ray fibre diffraction analysis of two heavy-atom derivatives. *J. Mol. Biol.* **149**, 675-707.
- [13] Marvin, D. A., Bryan, R. K. & Nave, C. (1987) Pf1 Inovirus. Electron density distribution calculated by a maximum entropy algorithm from native fibre diffraction data to 3 Å resolution and single isomorphous replacement data to 5

Å resolution. *J. Mol. Biol.* **193**, 315-343.

[14] Marvin, D. A., Hale, R. D., Nave, C. & Helmer-Citterich, M. (1994) Molecular models and structural comparisons of native and mutant class I filamentous bacteriophages Ff (fd, f1, M13), If1 and Ike. *J. Mol. Biol.* **235**, 260-286.

[15] Welsh, L. C., Symmons, M. F. & Marvin, D. A. (2000) The molecular structure and structural transition of the α -helical capsid in filamentous bacteriophage Pf1. *Acta Crystallog. sect. D* **56**, 137-150.

[16] Watts, T. H. (1983). Structure and Assembly of Pseudomonas Pili, Ph.D. Thesis, University of Alberta.

[17] Watts, T. H., Kay, C. M. & Paranchych, W. (1983) Spectral properties of three quaternary arrangements of Pseudomonas pilin. *Biochemistry* **22**, 3640-3646.

[18]. Kleywegt, G. J. & Jones, T. A. (1994). Detection, delineation, measurement and display of cavities in macromolecular structures. *Acta Crystallogr. sect. D* **50**, 178-185.

[19] Marvin, D.A. (1990) Model-building studies of Inovirus: genetic variations on a geometric theme. *Int. J. Biol. Macromol.* **12**, 125-138.

[20] Wright, P. E. & Dyson, H. J. (1999) Intrinsically

unstructured proteins: Re-assessing the protein structure-function paradigm. *J. Mol. Biol.* **293**, 321-331.

[21] Mahadevan, L. & Matsudaira, P. (2000) Motility powered by supramolecular springs and ratchets. *Science* **288**, 95-99.

[22] Marvin, D. A. & Wachtel, E. J. (1976) Structure and assembly of filamentous bacterial viruses. *Phil. Trans. Roy. Soc. Ser. B* **276**, 81-98.

[23] Opalka, N., Beckmann, R., Boisset, N., Simon, M. N., Russel, M. & Darst, S. A. (2003) Structure of the filamentous phage pIV multimer by cryo-electron microscopy. *J. Mol. Biol.* **325**, 461-470.

[24] Vainshtein, B. K. (1966) *Diffraction of X-rays by Chain Molecules*, Elsevier, Amsterdam.

[25] Inouye, H. (1994) X-ray scattering from a discrete helix with cumulative angular and translational disorders. *Acta Crystallogr. sect. A* **50**, 644-646.

[26] Guex, N. & Peitsch, M. C. (1997) SWISS-MODEL and the Swiss-PdbViewer: An environment for comparative protein modelling. *Electrophoresis* **18**, 2714-2723.